Second-generation HIF-activated oncolytic adenoviruses with improved replication, oncolytic, and anti-tumor efficacy

Tiffani Cherry[1,3], **Sharon L. Longo**[1], **Zulma Tovar-Spinoza**[1], and **Dawn E. Post**[1,2,4]

[1]Department of Neurosurgery, State University of New York (SUNY), Upstate Medical University, Syracuse New York

[2]Department of Microbiology & Immunology, State University of New York (SUNY), Upstate Medical University, Syracuse New York

[3]Department of Clinical Laboratory Sciences, State University of New York (SUNY), Upstate Medical University, Syracuse New York

Abstract

There is a need to develop more potent oncolytic adenoviruses that exhibit increased anti-tumor activity in patients. The HYPR-Ads are targeted oncolytic adenoviruses that specifically kill tumor cells which express active hypoxia-inducible factor (HIF). While therapeutically efficacious, the HYPR-Ads exhibited attenuated replication and oncolytic activity. To overcome these deficiencies and improve anti-tumor efficacy, we created new HIF-activated oncolytic Ads, HIF-Ad and HIF-Ad-IL4, which have two key changes: (i) a modified HIF-responsive promoter to regulate the E1A replication gene and (ii) insertion of the E3 gene region. The HIF-Ads demonstrated conditional activation of E1A expression under hypoxia. Importantly, the HIF-Ads exhibit hypoxia-dependent replication, oncolytic, and cellular release activities and potent anti-tumor efficacy, all of which are significantly greater than the HYPR-Ads. Notably, HIF-Ad-IL4 treatment led to regressions in tumor size by 70% and extensive tumor infiltration by leukocytes resulting in an anti-tumor efficacy that is up to 6-fold greater than the HYPR-Ads, HIF-Ad, and wild-type adenovirus treatment. These studies demonstrate that treatment with a HIF-activated oncolytic adenovirus leads to a measurable therapeutic response. The novel design of the HIF-Ads represents a significant improvement compared to first-generation oncolytic Ads and has great potential to increase the efficacy of this cancer therapy.

Keywords

hypoxia; hypoxia-inducible factor (HIF); adenovirus; tumor; oncolytic; virotherapy; interleukin-4

[4]Correspondence should be addressed to DEP: SUNY Upstate Medical University, Department of Neurosurgery, 750 East Adams St., Rm 4117 IHP, Syracuse, NY, 13210. Phone: (315) 464-9370, Fax: (315) 464-5504, postd@upstate.edu.

Conflict of Interest

The authors declare no conflict of interest.

Introduction

A clinically important target for anti-tumor therapy is hypoxia-inducible factor (HIF) which is associated with resistance to apoptosis, chemotherapy, and radiotherapy and increased invasion/metastasis, angiogenesis, and patient mortality.[1],[2] HIF is a transcription factor that is expressed in a wide range of primary tumors, metastases, and cancer stem cells, whereas it is undetectable in normal, healthy tissues.[3-5] Tumor-specific activation of HIF occurs by two mechanisms. First, HIF is activated in response to decreased oxygen (hypoxia) within the tumor mass.[2],[6],[7] Second, HIF is activated under normoxia in tumor cells that have acquired genetic mutations in oncogene and tumor suppressor gene pathways.[8] The importance of HIF in tumor biology is further highlighted by studies which demonstrate that experimental manipulation of HIF levels in tumor models leads to changes in tumor growth, angiogenesis and metastasis.[9-17] Furthermore, HIF plays a critical role in the self-renewal, proliferation, survival, and tumor initiation potential of cancer stem cells.[5] Consistent with these functional studies, a large number of HIF-regulated genes have critical roles in promoting tumorigenesis.[18] These findings indicate that drugs which eradicate HIF-active tumor cells may be useful anti-tumor agents. However, the identification of HIF inhibitors has encountered major obstacles, since all of the drugs currently developed target pathways which regulate HIF rather than directly inhibiting HIF.[2]

Oncolytic adenoviruses (Ads) are a cancer therapy which utilize the cytolytic replication cycle of the virus to specifically kill tumor cells (oncolysis). A wild-type Ad cannot be used for cancer therapy because it lacks tumor-specificity and is toxic to normal healthy tissues. A number of genetic engineering strategies have been employed to specifically target the Ad cytolytic replication cycle to tumor cells, thereby creating oncolytic Ads.[19-22] One strategy involves transcriptional regulation of E1A expression, a gene which is essential for Ad replication. This has been achieved using promoters that are preferentially active in tumors compared to normal tissues. Three oncolytic Ads, *dl*1520, Ad5-CD/TK*rep*, and CV706, have demonstrated overall safety and modest anti-tumor activity in clinical trials.[23] While encouraging, these first-generation oncolytic Ads had deficiencies in their design which contributed to weak anti-tumor efficacy in patients.[23-26] This highlights the need to optimize the design of oncolytic Ads prior to clinical trial testing

To specifically target and kill HIF-active tumor cells, we exploit the differential activation of HIF-dependent gene expression in tumors versus normal tissue for the design of HIF-activated oncolytic Ads. In the HIF-activated oncolytic Ad, HYPR-Ad#1, a novel bi-directional HIF-responsive promoter was introduced into the Ad genome for the regulated expression of E1A.[27],[28] Infection of tumor cells with HYPR-Ad#1 results in conditional E1A expression, viral replication, and tumor cell death under HIF-active conditions.[28] Importantly, HYPR-Ad#1 replicates in hypoxic regions of tumors *in vivo* and has anti-tumor activity resulting in a modest reduction in tumor growth.[29] To increase the anti-cancer efficacy of HYPR-Ad beyond the killing of HIF-active tumor cells, we armed the virus with the interleukin-4 (IL4) gene. IL4 was chosen because it is a potent multimodal anti-tumorigenic cytokine.[30] In HYPR-Ad-IL4, the bi-directional HIF-promoter is used for the co-regulated expression of E1A and IL4. HYPR-Ad-IL4 exhibits HIF-dependent E1A and IL4 expression, viral replication, and tumor cell lysis.[31] Importantly, HYPR-Ad-IL4

treatment results in rapid and long-lasting tumor regressions and its anti-tumor activity is superior to HYPR-Ad#1. Our studies with HYPR-Ad#1 and HYPR-Ad-IL4 provided critical proof that using a HIF-activated oncolytic adenovirus to kill HIF-active tumor cells and inhibit tumor growth is a feasible approach.[28],[29],[31] While promising, these viruses demonstrated decreased viral replication, oncolytic, and cellular release activity when compared to a wild type Ad *in vitro*.[31] It is important to correct these deficiencies prior to clinical studies since it impacts anti-tumor potency. The rationale is that increased viral progeny production (replication) and cell-to-cell spread (oncolysis and cellular release) will result in a more potent anti-tumor response. In this study, we created second-generation HIF-activated oncolytic Ads called HIF-Ad and HIF-Ad-IL4 which have two key genetic modifications that dramatically improve their replication, oncolytic, and anti-tumor efficacy compared to the HYPR-Ads. We anticipate that these improvements will translate into increased clinical efficacy and improved survival for cancer patients using oncolytic Ad therapy.

Results

The Ad replication cycle further increases HIF transcriptional activity under hypoxia

One potential explanation for the attenuated phenotype of the HYPR-Ads is an inhibition of the HIF pathway during the Ad replication cycle.[32],[33] Indeed, a large number of cellular pathways are dysregulated during the Ad replication cycle.[34] Therefore, we evaluated if HIF transcriptional activity was modulated under normoxia or hypoxia following infection with a wild-type Ad in LN229 (Figure 1a) and U251MG-T2 (Figure 1b) cells. For this, cells were transfected with a plasmid containing the luciferase reporter gene under the control of the same HIF-responsive promoter which is present in the HYPR-Ads. As expected[27], in mock infected cells there was a hypoxia-dependent increase in luciferase reporter gene expression ($p < 0.006$). In virus infected cells maintained under normoxia, the overall levels of HIF transcriptional activity remained relatively constant compared to mock infected cells ($p > 0.46$). An exception was a slight, but significant, 1.5 fold increase in HIF transcriptional activity in LN229 cells at multiplicity of infection (MOI) 25 ($p = 0.013$). In virus infected cells maintained under hypoxia, there was a dose-dependent increase in HIF transcriptional activity following virus infection compared to mock infected controls ($p < 0.013$). These results demonstrate that the Ad replication cycle further increases HIF transcriptional activity under hypoxia rather than inhibiting its activity. Therefore, we sought an alternative explanation for the reduced replication and oncolytic activity of the HYPR-Ads compared to a wild type Ad.

Construction of genetically-modified HYPR-Ads: HIF-Ad and HIF-Ad-IL4

We next evaluated whether genetic modifications to the HYPR-Ad genome would result in improved therapeutic efficacy. For this, we constructed genetically modified viruses called HIF-Ad and HIF-Ad-IL4 which have two important modifications compared to the HYPR-Ads: (i) substitution of a CMV- for a more efficient E1A- minimal promoter sequence in the right arm of the bi-directional HIF-promoter used to regulate E1A gene expression and (ii) insertion of the Ad E3 gene region (Figure 2a). In HIF-Ad-IL4, the IL4 adjuvant therapeutic gene was introduced into the left arm of the HIF-promoter. The HYPR-Ads contain a bi-

directional HIF-responsive promoter which consists of two genetically identical CMV minimal promoters that have the potential to form an inverted DNA repeat.[27],[28],[31] These repeats are associated with the formation of highly stable secondary structures, such as a cruciform or hairpin, which block DNA synthesis [reviewed in [35]-[37]]. Therefore, substituting a HRE-E1A promoter for one of the HRE-CMV promoters should allow us to circumvent this potential issue and lead to improved virus replication. The HYPR-Ads also have a deletion of the E3 gene region.[28],[31] The E3 region encodes the Adenovirus Death Protein (ADP) gene which plays a key role in host cell lysis and viral release at the completion of the Ad replication cycle.[38] Ads that lack ADP display impaired virus release, delayed cytolysis, slower cell-to-cell spread, and reduced anti-tumor activity compared to Ads that retain the ADP gene.[38],[39] Therefore, the inclusion of E3 in the HIF-Ads should lead to improved oncolysis and viral release. Below, we directly compare the therapeutic efficacy of the HIF-Ads versus the HYPR-Ads.

Hypoxia-dependent E1A and IL4 expression by HIF-Ad and HIF-Ad-IL4

Hypoxia-dependent regulation of the bi-directional HIF-responsive promoter within HIF-Ad and HIF-Ad-IL4 was examined by measuring E1A and IL4 protein expression under normoxia versus hypoxia. E1A expression was detected by western blot analysis using infected LN229 (Figure 2b) and Daoy (Supplementary Figure S1a) cell lysates. Mock infected cells served as a negative control and displayed no expression of E1A. Cells infected with Ad5WT, a wild-type Ad that lacks tumor-specificity and is not hypoxia regulated, displayed similar levels of E1A expression under normoxia and hypoxia. In contrast, HIF-Ad and HIF-Ad-IL4 displayed hypoxia-dependent E1A expression. Consistent with published studies[31], HYPR-Ad#1 and HYPR-Ad-IL4 also exhibited hypoxia-dependent E1A expression (Figure 2b). Of importance, the levels of E1A expression by the HIF-Ads under hypoxia were comparable to Ad5WT, demonstrating the strength of the HIF-responsive promoter.

IL4 expression by HIF-Ad-IL4 was measured by ELISA using conditioned media from virus infected LN229 (Figure 2c, d) and Daoy (Supplementary Figure S1b) cells. As expected, mock and HIF-Ad infected negative control samples showed undetectable IL4 levels under normoxia and hypoxia. In contrast to these controls, HIF-Ad-IL4 infected cells demonstrated a significant increase in the amount of IL4 produced under hypoxia versus normoxia. In agreement with published studies[31], HYPR-Ad-IL4 also exhibited hypoxia-dependent IL4 expression (Figure 2c, d). Under hypoxia there was no difference in the amount of IL4 produced in HIF-Ad-IL4 versus HYPR-Ad-IL4 infected cells at 2 dpi (1.3-fold increase; p= 0.951, Figure 2c). In contrast, at 4 dpi there was a significant 5-fold increase in the amount of IL4 produced under hypoxia by HIF-Ad-IL4 compared to HYPR-Ad-IL4 infected cells (p< 0.001, Fig. 2d).

In summary, these results demonstrate that HIF-Ad and HIF-Ad-IL4 express E1A and IL4 selectively under hypoxia and that the bi-directional HIF-responsive promoter maintains its proper regulation in the HIF-Ad genome.

The HIF-Ads have dramatically improved hypoxia-dependent oncolytic activity compared to the HYPR-Ads

The ability of HIF-Ad and HIF-Ad-IL4 to specifically lyse hypoxic tumor cells was evaluated in LN229 (Figure 3a), Daoy (Supplementary Figure S1c), and U251MG-T2 (Supplementary Figures S2) tumor cells. Mock and replication-deficient AdLacZ infected cells served as negative controls and displayed less than 1% cell death under normoxia and hypoxia. This demonstrates the lack of toxicity due to Ad infection and/or hypoxic conditions. Ad5WT induced extensive cytolysis under normoxia and hypoxia. In contrast, all of the HIF-activated Ads (HIF-Ad, HIF-Ad-IL4, HYPR-Ad#1, and HYPR-Ad-IL4) induced hypoxia-dependent tumor cell lysis. Of importance, a difference in the rate and magnitude of cytopathic effect (CPE) was noted between the HIF-Ads and the HYPR-Ads. In the LN229 study, under hypoxia the HIF-Ads induced extensive CPE at MOI 10 while the HYPR-Ads did not induce CPE until MOI 25 (Figure 3a). In the U251MG-T2 study, HIF-Ad and HIF-Ad-IL4 showed extensive cell death under hypoxia at MOI 0.25, 1, and 3 by day 6 (Supplementary Figure S2a). In contrast, HYPR-Ad#1 and HYPR-Ad-IL4 began to induce cell death under hypoxia at only MOI 3 by day 8 (Supplementary Figure S2b). Quantitative MTT assays independently confirmed that the cytopathic effect of the HIF-Ads was significantly greater than the HYPR-Ads under hypoxia (Figure 3b and Supplementary Figure S3, $p<0.001$). In addition, the cytolytic activity of the HIF-Ads under hypoxia was similar to that obtained with Ad5WT, demonstrating the potent tumor-specific cytolytic activity of the HIF-Ads (Figure 3c and Supplementary Figure S1d, $p>0.58$). Collectively, these results demonstrate that the HIF-Ads have hypoxia-dependent oncolytic activity which is significantly improved compared to the HYPR-Ads.

The HIF-Ads have significantly improved hypoxia-dependent replication compared to the HYPR-Ads

The efficiency of HIF-Ad and HIF-Ad-IL4 replication under normoxia versus hypoxia was examined in LN229 (Figure 4a, b) and Daoy (Supplementary Figure S1e) cells. All of the HIF-activated Ads displayed hypoxia-dependent replication. A prominent difference between the HIF-Ads and the HYPR-Ads was that the HIF-Ads had a large increase, 51-664 fold, in virus production under hypoxia versus normoxia. Consistent with published studies[31], the fold-increase in HYPR-Ad replication under hypoxia versus normoxia was more modest, 6-22 fold. Importantly, the HIF-Ads have significantly greater hypoxia-dependent replication than the HYPR-Ads (6-17 fold increase, $p<0.001$).

The replication of the HIF-Ads was also compared to Ad5WT in LN229 (Figure 4a, b) and Daoy (Supplemental Figure S1e) cells. As expected, the replication of Ad5WT was not hypoxia regulated. In the LN229 study, Ad5WT displayed a 2-5 fold increase in replication compared to HIF-Ad (Figure 4a) and HIF-Ad-IL4 (Figure 4b) under hypoxia ($p<0.013$). In the Daoy study, there was no significant difference in the replication of the HIF-Ads compared to Ad5WT under hypoxia (Supplementary Figure S1e, $p>0.054$). These results differ greatly from the 14-77 fold decrease in HYPR-Ad#1 (Figure 4a) and HYPR-Ad-IL4 (Figure 4b) replication compared to Ad5WT under hypoxia ($p<0.006$). These data demonstrate that the gap in virus replication between the HYPR-Ads and a wild type Ad has been greatly reduced in the HIF-Ads.

The HIF-Ads have dramatically improved hypoxia-dependent cellular release compared to the HYPR-Ads

Given the important role of the Ad death protein (ADP) in cell lysis and virus release[38], we examined the release of HIF-Ad and HIF-Ad-IL4 from infected LN229 (Figure 4c, d) and Daoy (Supplementary Figure S1f) cells under normoxia versus hypoxia. HIF-Ad and HIF-Ad-IL4 displayed a large increase in cellular release under hypoxia compared to normoxia (224-326 fold in LN229 and 19-42 fold in Daoy cells, p<0.002). HYPR-Ad#1 (Figure 4c) and HYPR-Ad-IL4 (Figure 4d) also exhibited hypoxia-dependent cellular release, although the induction under hypoxia versus normoxia was a modest 4-fold (p>0.064). Notably, the HIF-Ads have dramatically improved hypoxia-dependent cellular release than the HYPR-Ads (97-870 fold increase, p<0.002). This is consistent with the presence of the ADP gene in the HIF-Ads and its absence from the HYPR-Ads.

The cellular release of the HIF-Ads was also compared to Ad5WT using LN229 (Figure 4c, d) and Daoy (Supplementary Figure S1f) cells. The cellular release of Ad5WT was not hypoxia regulated. Additionally, the cellular release of Ad5WT was 2-8 fold greater than HIF-Ad and HIF-Ad-IL4 under hypoxia (p<0.003). In contrast, under hypoxia HYPR-Ad#1 (Figure 4c) and HYPR-Ad-IL4 (Figure 4d) showed a 219-6740 fold decrease in cellular release compared to Ad5WT (p<0.001). These results show that the large difference in cellular release between the HYPR-Ads and wild type Ads is significantly diminished in the HIF-Ads.

The HIF-Ads have potent anti-tumor activity which is superior to the HYPR-Ads

The anti-tumor efficacy of HIF-Ad and HIF-Ad-IL4 was examined in two independent studies using subcutaneous LN229 tumor xenografts in *nu/nu* mice (Figure 5a, b). In Study 1, tumors were grown to an average size of 92mm^3 and then treated intratumorally with HIF-Ad-IL4, Ad5WT, or PBS (Figure 5a). Tumor growth was monitored for 45 days post-treatment at which point the PBS-treated tumors exhibited a 9.5-fold increase in size and tumor burden was reached. In contrast, Ad5WT and HIF-Ad-IL4 treatment led to a dramatic 8.6- to 19-fold reduction in tumor growth, respectively, compared to PBS-treated tumors (p<0.001). Quite striking was the large number of tumors which exhibited a regression in size following HIF-Ad-IL4 and Ad5WT treatment (Supplemental Table S1). For example, by Day 71 of the study (45 day post-treatment), there were 9/10, 7/10, and 1/10 tumors which exhibited a regression in size following HIF-Ad-IL4, Ad5WT, and PBS treatment, respectively. In addition, the magnitude of the tumor regressions were dramatic with HIF-Ad-IL4- and Ad5WT- treated tumors exhibiting an average 70% regression in size (not shown). Finally, tumor growth inhibition by HIF-Ad-IL4 and Ad5WT treatment was maintained long-term. In Study 2, the anti-tumor efficacy analysis was expanded to include HIF-Ad treatment and the ability to inhibit the growth of large tumors (Figure 5b). Tumor xenografts were grown to an average size of 235 mm^3 and then treated intratumorally with HIF-Ad, HIF-Ad-IL4, Ad5WT, or PBS. Tumor growth was monitored for 28 days post-treatment when animals had to be sacrificed due to the large size of the PBS-treated tumors. During this period, an 8-fold increase in tumor size was seen in the PBS treatment group. HIF-Ad and Ad5WT treatment led to a modest 2-fold reduction in tumor growth compared to PBS treated tumors (p=0.045 and p=0.047, respectively). There was no evidence of tumor

regressions in the PBS, HIF-Ad and Ad5WT treatment groups (Supplemental Table S2). In striking contrast, all of the tumors treated with HIF-Ad-IL4 (4/4) showed a regression in tumor size by 40-85% (Supplemental Table S2). At the end of the study there was a significant 12-fold reduction in tumor growth in the HIF-Ad-IL4 treatment group compared to PBS-treated tumors (p=0.003). Finally, there were no virus treatment-related deaths or observable toxicity (activity or weight change) in these two animal tumor studies (Supplemental Figure S4a, b). These data illustrate that HIF-Ad and HIF-Ad-IL4 have potent anti-tumor activity which is equal to or greater than Ad5WT.

The anti-tumor efficacy of the HIF-Ads was also compared to the HYPR-Ads using subcutaneous LN229 tumor xenografts in *nu/nu* mice (Figures 5c, d). In the first study, tumors were treated intratumorally with HIF-Ad, HYPR-Ad#1, or PBS at a viral dose of 5×10^7 (Figure 5c) or 5×10^6 (Supplemental Figure 5) IFU, which are 4- and 40- fold lower than the dose used in Figure 5b. In the second study, tumors were treated with HIF-Ad-IL4, HYPR-Ad-IL4, or PBS at a viral dose of 1×10^6 IFU (Figure 5d), which is 200-fold lower than the dose used in Figure 5a and Figure 5b. In both studies, tumor growth was monitored for approximately 4-weeks post-treatment when animals had to be sacrificed due to the large size of the PBS- and HYPR-Ad- treated tumors. There were no virus treatment-related deaths or observable toxicity (activity or weight change) in these two animal tumor studies (Supplemental Figure S4c, d). PBS-treated tumors exhibited a continuous increase in tumor growth. Treatment with HYPR-Ad#1 and HYPR-Ad-IL4 did not reduce tumor growth (p>0.087). In contrast, HIF-Ad and HIF-Ad-IL4 treatments inhibited tumor growth even at the low viral dose used. HIF-Ad treatment at the 5×10^7 IFU dose led to a significant 1.8-3.2 fold decrease in tumor growth compared to PBS- and HYPR-Ad#1- treated tumors from Day 49 to Day 64 of the study (**Figure 5c**, p<0.039). These results demonstrate that the augmented replication and cytolytic activity of HIF-Ad measured *in vitro* translated into an improved anti-tumor response. HIF-Ad-IL4 treatment resulted in a significant 1.5-2.3 fold decrease in tumor growth compared to PBS- and HYPR-Ad-IL4- treated tumors from Day 52 to Day 73 of the study (**Figure 5d**, p<0.005). The HIF-Ad-IL4 versus HYPR-Ad-IL4 study was repeated with similar findings (not shown). However, treatment with HIF-Ad at the 5×10^6 IFU dose did not reduce tumor growth (Supplemental Figure 5). These results indicate that the observed anti-tumor response of HIF-Ad-IL4 at the 1×10^6 IFU dose is most likely due to expression of the IL4 therapeutic gene rather than the cytolytic activity of the virus. In summary, these results demonstrate that the anti-tumor activity of the HIF-Ads is superior to the HYPR-Ads.

To better understand the potent anti-tumor effects of HIF-Ad-IL4 compared to HIF-Ad and HYPR-Ad-IL4, we examined intratumoral IL4 levels and tumor infiltration by CD45+ leukocytes (Figure 6). Intratumoral IL4 levels were measured in LN229 tumors treated with HYPR-Ad-IL4 or HIF-Ad-IL4 (Figure 6a). HIF-Ad-IL4 treated tumors showed a significant 2- and 27- fold increase in intratumoral IL4 levels compared to HYPR-Ad-IL4 treated tumors at Days 4 and 10 post treatment, respectively (p<0.018). In an independent experiment, we included HIF-Ad treatment for comparison (Figure 6b). In this study, tumors treated with HIF-Ad-IL4 showed a 9-10 fold increase in intratumoral IL4 levels compared to HIF-Ad and HYPR-Ad-IL4 treated tumors at Day 11 post treatment (p<0.033). Importantly,

there was no difference in intratumoral IL4 levels between HIF-Ad and HYPR-Ad-IL4 treated tumors (p=0.976). CD45 leukocyte common antigen immunostaining demonstrated that HIF-Ad-IL4 treated tumors contained extensive tumor infiltration by CD45+ leukocytes (Figure 6c). In contrast, PBS and HIF-Ad treated tumors contained CD45+ leukocytes, but the degree of infiltrate was substantially less compared to the HIF-Ad-IL4 treated tumor (Figure 6c). H&E staining showed that HIF-Ad-IL4 treatment leads to widespread immune cell infiltration and tumor necrosis with little viable tumor remaining (Figure 6c). In contrast, H&E staining of PBS- and HIF-Ad treated tumors showed mostly viable tumor (Figure 6c). PBS treated tumors had no necrosis whereas HIF-Ad treated tumors showed a small number of isolated necrotic pockets. These results demonstrate that HIF-Ad-IL4 expresses high levels of IL4 in treated tumors and this correlates with massive tumor infiltration by CD45+ leukocytes and tumor cell necrosis.

Discussion

The results show that we have successfully created two second-generation HIF-activated Ads, HIF-Ad and HIF-Ad-IL4, that have enhanced oncolytic properties. The use of an alternative Ad cloning system enabled the introduction of two key alterations in HIF-Ad and HIF-Ad-IL4: (i) a modified HIF-responsive promoter to enhance virus replication and (ii) insertion of the E3 gene region to enhance the spread of the virus through the tumor. As a result HIF-Ad and HIF-Ad-IL4 have robust hypoxia/HIF-dependent E1A and IL4 expression, replication, cellular release, and oncolytic activity. In addition, these viruses have anti-tumor activity. Most importantly, the HIF-Ads have significantly increased replication, cellular release, oncolytic, and anti-tumor activity compared to the first-generation HYPR-Ad series of HIF-activated oncolytic Ads. These studies demonstrate the increased potency of the HIF-Ads for cancer therapy.

We were the first to describe the use of a bi-directional promoter to simultaneously regulate expression of E1A and a therapeutic transgene in an oncolytic Ad.[28],[31] The bi-directional HIF-responsive promoter that we designed is unique and offers several advantages compared to other promoters. First, the size of the promoter is relatively small. Second, the promoter is bi-directional. These features allow us introduce the exogenous promoter and a therapeutic transgene without the need to delete important viral genes, such as those in the E3 gene region. An alternative strategy is to incorporate large exogenous promoters and/or therapeutic transgenes following a complete or partial deletion of the E3 gene region.[19],[40]-[42] One drawback to this approach is accelerated virus clearance by the host immune response *in vivo*.[43] A third important feature of our HIF-responsive promoter is that it is not inhibited during the Ad replication cycle (Figure 1). E1A can bind to the p300 transcriptional co-activator resulting in an inhibition of HIF-dependent gene expression.[32],[33] However, a number of HIF-target genes are still activated in the absence of p300.[44] Given the complex regulation of HIF transcriptional activity[45], it is possible that the specific configuration of our HIF-responsive promoter confers a p300-independent activation mechanism. Alternatively, the ability of E1A to abrogate HIF-dependent gene expression may be dependent upon the E1A and/or p300 levels which are present in a particular model or experimental condition. A fourth advantage of our HIF-responsive promoter is its ability to retain selective activation in response to hypoxia following its incorporation into the Ad

genome (Figure 2). In contrast, an alternative HIF-responsive promoter lost its hypoxia-dependent regulation when introduced into the Ad genome.[46] Finally, our results show the HIF-Ads expressed similar E1A levels under hypoxia compared to a wild-type Ad (Figures 2b and S1a). This demonstrates that the transcriptional strength of the HIF-responsive promoter present within the HIF-Ads is similar to the endogenous E1A promoter of a wild-type Ad. Consistent with this, the levels of E1A induced under hypoxia efficiently activate the HIF-Ad replication cycle (Figures 4a, b and S1e). This results in extensive killing of hypoxic, but not normoxic, tumor cells in culture (Figures 3 and S1d) and anti-tumor activity *in vivo* (Figure 5). These features of HIF-Ad are important since hypoxia can negatively effect the replication and oncolytic efficacy of wild-type Ads in culture.[47,48]

The rationale for improving HIF-activated oncolytic Ad therapy is that increased viral progeny production (replication) and cell-to-cell spread (oncolysis and cellular release) will result in a more potent anti-tumor response. Our results demonstrate that HIF-Ad has significantly improved replication, cytolysis, and cellular release compared to HYPR-Ad#1 *in vitro* and this leads to in an improved anti-tumor response *in vivo*. Our data also demonstrate increased expression of the IL4 transgene by HIF-Ad-IL4 compared to HYPR-Ad-IL4 *in vitro* and *in vivo*. These results are most likely due to increased replication of HIF-Ad-IL4 rather than differences in the strength of the HIF-responsive promoters. In support of this are the E1A expression and virus replication studies (Figures 2 and 4). To further address this, it will be important to conduct detailed *in vivo* viral replication and E1A and IL4 expression studies following HYPR-Ad#1, HIF-Ad, HYPR-Ad-IL4, and HIF-Ad-IL4 treatments.

The IL4 cytokine has multimodal anti-tumor activity associated with its ability to induce a host anti-tumor immune response, inhibit tumor angiogenesis, and inhibit tumor cell proliferation.[30] Our studies demonstrate the potent anti-tumor effect of IL4 when locally delivered to the tumor microenvironment by an oncolytic Ad. Furthermore, we demonstrate that the intrinsic oncolytic effect of HIF-Ad and the actions of the IL4 transgene are important components of the anti-tumor effect. The data also suggest that the anti-tumor effects of IL4 are stronger than the oncolytic activity of the virus. Now that we have established the anti-tumor efficacy of HIF-Ad and HIF-Ad-IL4 it will be important to better understand the mechanism(s) underlying the potent anti-tumor response induced by IL4. Here we demonstrate that HIF-Ad-IL4 treatment is associated with extensive infiltration of the tumor mass with CD45+ leukocytes. A next useful study will be to identify and quantify the specific immune cell types which are infiltrating the tumors in response to IL4 expression versus oncolytic Ad treatment. Once this is defined, we can determine the role of the host immune response in the anti-tumor activity of HIF-Ad-IL4. In addition to gaining a better understanding of how IL4 modulates host immune responses, we can also explore whether IL4 induces an anti-angiogenic response in our tumor models. This may be particularly advantageous for HIF-Ad treatment because it would generate hypoxia/HIF-activation in the tumor mass, thereby creating a positive feedback loop leading to increased activation of the virus. Finally, additional anti-tumor efficacy studies using recently identified syngeneic rodent tumor models that support human Ad replication will be highly beneficial.[49-52] These tumor models utilize immunocompetent rodents that have a fully

functional immune system and therefore will enable us to evaluate T- and B- cell responses during HIF-Ad treatment. However, the use of IL4 for cancer therapy is controversial because it may not support a strong, long-term immunity mediated by CD8+ cytolytic T-lymphocytes (CTL). On the other hand, the ability of IL4 to suppress a Th1 type anti-viral immune response mediated by CTL may be beneficial for HIF-Ad therapy by reducing virus clearance.[53-55] This may lead to prolonged intratumoral virus replication and greater tumor cell death. Regardless of the mechanism, our studies with HIF-Ad-IL4 and published studies on IL4 treatment of experimental tumors demonstrate that IL4 can induce regressions in tumor size and tumor eradication. [31,56,57] This justifies the continued pursuit of the IL4 cytokine for cancer therapy.

Our results demonstrate that the replication and oncolytic efficacy of the HIF-activated oncolytic Ads has been increased without compromising tumor-specificity. For comparison, we utilized a wild-type Ad (Ad5WT) which is not tumor selective and therefore cannot be used in a clinical setting due to widespread toxicity to normal, healthy cells. We found that the HIF-Ads have hypoxia-dependent replication which is similar to or slightly reduced compared to Ad5WT. In addition, the HIF-Ads induced hypoxia-dependent cytotoxicity at a rate and magnitude that was indistinguishable from Ad5WT. Finally, the HIF-Ads exhibited anti-tumor activity which was similar to or greater than Ad5WT. In the case of large tumors, the anti-tumor efficacy of HIF-Ad-IL4 was superior to Ad5WT. Most importantly, the anti-tumor activity of HIF-activated oncolytic Ad treatment was improved without increasing general toxicity (changes in animal weight or behavior). In contrast, an oncolytic Ad which expresses IL12 (induces a classical Th1 type immune response) caused toxicity in rodents which required a reduction in the viral dose for *in vivo* studies.[58] Toxicity was due to IL12 expression, not viral replication. Our *in vivo* studies with HIF-Ad-IL4 demonstrate that therapeutically efficacious levels of IL4 can be achieved and these cytokine levels do not cause obvious signs of toxicity in treated rodents compared to PBS or HIF-Ad treatment. The next step is to undertake extensive safety and toxicity studies of the HIF-Ads *in vivo* using permissive animal models. Recently, the ability of the cotton rat[59] and Syrian golden hamster[60] to support human Ad replication was demonstrated. The use of these animal models will allow us to better evaluate if the HIF-Ads replicate in a particular organ/tissue or under certain *in vivo* conditions.

Collectively, our data demonstrates that we have developed a potent and efficacious HIF-activated oncolytic Ad for the treatment of hypoxic tumor cells. Since hypoxia is a hallmark of tumor growth and progression, the HIF-Ads can be used as a treatment for a wide range of primary and metastatic tumors regardless of tissue origin or genetic mutations in oncogene and tumor suppressor gene pathways.

Materials & Methods

Construction of HIF-Ad and HIF-Ad-IL4, adenoviruses, and cells

HIF-Ad and HIF-Ad-IL4 were created using the pE1.1 and pAd329 vectors (OD260, Inc., Boise, ID). To generate HIF-Ad, an 884-bp SpeI/StuI fragment from pBI-V6R[27] was ligated into the shuttle vector pE1.1 digested with XbaI/EcoRV, creating pE1.1-V6R. pE1.1-V6R was digested with DraIII and ligated into the SfiI pre-digested pAd329 vector, creating pAd-

V6R. To generate HIF-Ad-IL4, a 1326-bp SpeI/StuI fragment from pBI-V6R-IL4[31] was ligated into pE1.1 digested with XbaI/EcoRV, creating pE1.1-V6R-IL4. pE1.1-V6R-IL4 was digested with DraIII and ligated into the SfiI pre-digested pAd329 vector, creating pAd-V6R-IL4. To create recombinant HIF-Ad and HIF-Ad-IL4 viruses, pAd-V6R and pAd-V6R-IL4 were transferred into E. coli via packaging into phage λ to create pAd cosmids. pAd cosmids were linearized with PacI and then purified using the Qiaex II kit (Qiagen, Valencia, CA). Ad293 packaging cells were transfected with linearized pAd cosmid using lipofectamine (Invitrogen, Carlsbad, CA) and then incubated in a standard cell culture incubator until viral plaques were observed (eight-nine days). Virus was recovered from cells by three freeze-thaw cycles.

AdLacZ is a replication deficient Ad which lacks the E1 gene region and expresses LacZ (UNC Virus Vector Core Facility, Chapel Hill, NC). Ad5WT is a replication-competent Ad which contains a wild-type E1 and E3 gene regions (OD260, Inc.). HYPR-Ad#1[29] and HYPR-Ad-IL4[31] are HIF-activated oncolytic Ads which contain the E1A gene under the regulation of a bi-directional HIF-responsive promoter and a deleted E3 gene region. Large-scale amplification and purification of Ad5WT, HYPR-Ad#1, HYPR-Ad-IL4, HIF-Ad, and HIF-Ad-IL4 stocks was performed by OD260, Inc. Prior to use, all virus stocks were titered as described in [31].

Human LN229 glioma[61], U251MG-T2 glioma[29], Daoy medulloblastoma (ATCC, Manassas, VA), and Ad293 embryonic kidney (Stratagene, La Jolla, CA) cells were cultured in DMEM containing 10% FCS under normoxia. Normoxic (21% O_2) and hypoxic (1% O_2) cell culture conditions were generated as described in [29]. LN229, U251MG-T2, and Daoy cells were selected because they have a hypoxia-activated HIF-pathway.[28]

HIF transcriptional activity

HIF transcriptional activity was measured using a luciferase reporter gene assay. LN229 (2.25×10^5) and U251MG-T2 (1.25×10^5) cells were transfected with 1 µg pBIGL-V6R using GenePORTER transfection reagent (Genlantis, San Diego, CA) as described in [27]. pBIGL-V6R contains the luciferase reporter gene under the control of a HIF-responsive promoter. The next day, cells were mock or virus infected with a wild-type Ad (dl309-Ad, UNC Virus Vector Core Facility) in triplicate. LN229 cells were infected at MOI 1, 5, and 25 while U251MG cells were infected at MOI 0.0625, 0.25, and 1. Cells were placed under normoxia versus hypoxia. One day later luciferase activity was measured using a Luc-screen kit (Applied Biosystems, Foster City, CA) and normalized to total cellular protein (light units/µg protein).

E1A and IL4 expression

LN229 and Daoy cells were mock or virus infected at MOI 1. The cells were placed under normoxia versus hypoxia. E1A expression was examined by western blot analysis. Cells were collected in PBS using a cell scraper and then pelleted by microcentrifugation for 5 minutes at 2300 × g. Collected cells were lysed using lysing buffer [20 mM Sodium Phosphate, 5mM EDTA, 150mM NaCl, 50mM NaF, 1% Triton X-100, 1X protease inhibitor cocktail and 1X phosphatase inhibitor cocktail (Sigma, St. Louis, MO)]. Protein

concentrations were determined using Protein Assay Dye (BioRad, Hercules, CA). Proteins (15 or 20ug) were separated by electrophoresis using 10% Criterion Precast gels (BioRad) and blotted to PVDF membrane (BioRad). The primary antibody was anti-E1A (Adenovirus Ab-5 cocktail, NeoMarkers, Fremont, CA). The secondary antibody was anti-mouse IgG + IgM alkaline phosphate linked whole antibody from goat (Amersham Biosciences, Piscataway, NJ). Signal was detected using ECF substrate (Amersham Biosciences). The membrane was stripped of signal using 1X Stripping buffer (Boston BioProducts, Worcester, MA) and then reprobed with the primary antibody anti-GAPDH (Calbiochem, La Jolla, CA) as a loading control. IL4 protein levels were quantified by ELISA (Pierce, Rockford, IL) using conditioned media collected from *in vitro* studies or tumor homogenates from *in vivo* studies. For the intratumoral IL4 expression studies, LN229 cells (7.5×10^6 cells in 200ul PBS) were implanted subcutaneously into the flanks of *nu/nu* mice (athymic NCr-nu, NCI, Frederick, MD). In Figure 6a, tumors were established to an average size of 223 mm^3 and then injected intratumorally with 5×10^5 infectious forming units (IFU) of HIF-Ad-IL4 or HYPR-Ad-IL4 diluted in PBS (0.1 ml total injection volume). Tumors (n=5 mice/group) were collected on Days 4 and 10 post-treatment. In Figure 6b, tumors were established to an average size of 132 mm^3 and then injected intratumorally with 5×10^5 infectious forming units (IFU) of HIF-Ad, HIF-Ad-IL4, or HYPR-Ad-IL4. Tumors (n=6 mice/group) were collected at Day 11 post-treatment. Collected tumors were homogenized in 0.75ml PBS, sonicated for one minute, centrifuged for 5 minutes at $16,000 \times g$ at 4°C, and the cleared supernatant used for ELISA. Intratumoral IL4 levels were normalized to total protein levels (BioRad, Protein Assay Dye) of the cleared tumor homogenates.

Tumor cell lysis assays

For CPE assays, LN229 cells were infected at MOI 10 and 25; U251MG-T2 cells were infected at MOI 0.25, 1, and 3; and Daoy were infected at MOI 5. For 3-(4,5 dimethlyliazol-2-yl)-2,5 diphenyltetrazolium bromide (MTT) assays, LN229 cells were infected at MOI 25 while U251MG-T2 cells were infected at MOI 0.25 and 1.0 in triplicate. For lactate dehydrogenase (LDH) assays, LN229 cells were infected at MOI 25 while Daoy cells were infected at MOI 1 in triplicate. Following infection, cells were placed under normoxia versus hypoxia. Cells were visually monitored for cytopathic effect (CPE) (cell lysis/detachment) and then analyzed when extensive CPE was seen in HIF-Ad/HIF-Ad-IL4 infected cells under hypoxia. For CPE assays, the cells were fixed with ice cold 100% methanol, stained with crystal violet solution (1% crystal violet, 10% formaldehyde, 20% ethanol, in water) for 20 min, destained in water, and allowed to dry at room temperature. Photographs were taken at 100X magnification. Cytopathic effect was quantified by a MTT assay. Cytotoxicity was quantified by a LDH assay (Cytotoxicity Detection Kit, Roche Applied Science, Indianapolis, IN). For the MTT and LDH assays, values obtained with virus infection were normalized to mock infected cells.

Viral replication and cellular release assays

LN229 and Daoy cells were infected with virus at MOI 1 in triplicate. The cells were placed under normoxia versus hypoxia. For the viral replication assay, cells were collected in PBS using a cell scraper and pelleted by microcentrifugation for 5 minutes at $16,000 \times g$. Cell pellets were resuspended in serum-free DMEM and virus was released from the cells by

three freeze-thaw cycles. Cellular debris was removed by microcentrifugation and the virus containing supernatant was titered as described in [31]. For the cellular release assay, conditioned media was collected and titered.

Anti-tumor efficacy Studies

LN229 cells (7.5×10^6 cells in 200ul PBS) were implanted subcutaneously into the flanks of *nu/nu* mice (athymic NCr-nu, NCI, Frederick, MD, Day 1 of the study). In Figure 5a, tumors were established to an average size of 92 mm^3 and then injected intratumorally with 2×10^8 IFU of virus (HIF-Ad-IL4, Ad5WT) or diluent (PBS, 0.075 total injection volume) on days 26 and 29. n=10 mice/group. In Figure 5b, tumors were established to an average size of 235 mm^3 and then injected intratumorally with 2×10^8 IFU of virus (HIF-Ad, HIF-Ad-IL4, Ad5WT) or PBS on days 28 and 34. n = 4 mice/group. In Figure 5c and Supplemental Figure 5, tumors were established to an average size of 110 mm^3 and then injected intratumorally with 5×10^7 (Figure 5c) or 5×10^6 (Supplemental Figure 5) IFU of HIF-Ad (n=9), HYPR-Ad#1 (n=9) or PBS (n=8) on days 35 and 39. In Figure 5d, tumors were established to an average size of 226 mm^3 and then injected intratumorally with 1×10^6 IFU of HIF-Ad-IL4 (n=8), HYPR-Ad-IL4 (n=9) or PBS (n=8) on days 45 and 49. Tumor size was measured with a digital caliper and tumor volume was calculated using the formula: [(length × width^2)/2]. All animal experiments were conducted according to IACUC guidelines for the care and use of experimental animals and were approved by the Institutional Committee for the Humane Use of Animals.

H&E and CD45+ leukocyte analysis of tumors

S.c. LN229 tumors in *nu/nu* mice were treated with PBS or 1×10^7 IFU of HIF-Ad or HIF-Ad-IL4 at Days 35 and 39 post-tumor cell implantation. On Day 49, tumors were harvested and processed for sectioning as described in [31]. Tumor sections were stained with H&E and immunostained for CD45 leukocyte common antigen, a pan leukocyte marker, as described in [31].

Statistical Analysis

ELISA, MTT, LDH, viral replication, and cellular release data was analyzed using a Students *t* test. In the tumor studies shown in Figures 5a-d, tumor volume was analyzed using a one way ANOVA and the Holm-Sidak test for pairwise comparison. For the intratumoral IL4 studies shown in Figures 6a and 6b, IL4 protein levels were analyzed by a t-test or one way ANOVA (Holm-Sidak test for pairwise comparison), respectively. A p<0.05 was considered statistically different.

Supplementary Material

Refer to Web version on PubMed Central for supplementary material.

Acknowledgements

Abbreviations

HIF	hypoxia-inducible factor
IL4	interleukin-4
MOI	multiplicity of infection
LDH	lactate dehydrogenase
CPE	cytopathic effect
IFU	infectious forming units
dpi	days post infection

References

1. Brown JM, Wilson WR. Exploiting tumour hypoxia in cancer treatment. Nat Rev Cancer. 2004; 4:437–447. [PubMed: 15170446]

2. Semenza GL. Evaluation of HIF-1 inhibitors as anticancer agents. Drug Discov Today. 2007; 12:853–859. [PubMed: 17933687]

3. Zhong H, De Marzo AM, Laughner E, Lim M, Hilton DA, Zagzag D, et al. Overexpression of hypoxia-inducible factor 1alpha in common human cancers and their metastases. Cancer Res. 1999; 59:5830–5835. [PubMed: 10582706]

4. Talks KL, Turley H, Gatter KC, Maxwell PH, Pugh CW, Ratcliffe PJ, et al. The expression and distribution of the hypoxia-inducible factors HIF-1alpha and HIF-2alpha in normal human tissues, cancers, and tumor-associated macrophages. Am J Pathol. 2000; 157:411–421. [PubMed: 10934146]

5. Li Z, Bao S, Wu Q, Wang H, Eyler C, Sathornsumetee S, et al. Hypoxia-inducible factors regulate tumorigenic capacity of glioma stem cells. Cancer Cell. 2009; 15:501–513. [PubMed: 19477429]

6. Weidemann A, Johnson RS. Biology of HIF-1alpha. Cell Death Differ. 2008; 15:621–627. [PubMed: 18259201]

7. Patel SA, Simon MC. Biology of hypoxia-inducible factor-2alpha in development and disease. Cell Death Differ. 2008; 15:628–634. [PubMed: 18259197]

8. Bardos JI, Ashcroft M. Negative and positive regulation of HIF-1: a complex network. Biochim Biophys Acta. 2005; 1755:107–120. [PubMed: 15994012]

9. Ravi R, Mookerjee B, Bhujwalla ZM, Sutter CH, Artemov D, Zeng Q, et al. Regulation of tumor angiogenesis by p53-induced degradation of hypoxia-inducible factor 1alpha. Genes Dev. 2000; 14:34–44. [PubMed: 10640274]

10. Stoeltzing O, McCarty MF, Wey JS, Fan F, Liu W, Belcheva A, et al. Role of hypoxia-inducible factor 1alpha in gastric cancer cell growth, angiogenesis, and vessel maturation. J Natl Cancer Inst. 2004; 96:946–956. [PubMed: 15199114]

11. Li L, Lin X, Staver M, Shoemaker A, Semizarov D, Fesik SW, et al. Evaluating hypoxia-inducible factor-1alpha as a cancer therapeutic target via inducible RNA interference in vivo. Cancer Res. 2005; 65:7249–7258. [PubMed: 16103076]

12. Hiraga T, Kizaka-Kondoh S, Hirota K, Hiraoka M, Yoneda T. Hypoxia and hypoxia-inducible factor-1 expression enhance osteolytic bone metastases of breast cancer. Cancer Res. 2007; 67:4157–4163. [PubMed: 17483326]

13. Liao D, Corle C, Seagroves TN, Johnson RS. Hypoxia-inducible factor-1alpha is a key regulator of metastasis in a transgenic model of cancer initiation and progression. Cancer Res. 2007; 67:563–572. [PubMed: 17234764]

14. Kondo K, Kim WY, Lechpammer M, Kaelin WG Jr. Inhibition of HIF2alpha is sufficient to suppress pVHL-defective tumor growth. PLoS Biol. 2003; 1:E83. [PubMed: 14691554]

15. Ryan HE, Poloni M, McNulty W, Elson D, Gassmann M, Arbeit JM, et al. Hypoxia-inducible factor-1alpha is a positive factor in solid tumor growth. Cancer Res. 2000; 60:4010–4015. [PubMed: 10945599]

16. Blouw B, Song H, Tihan T, Bosze J, Ferrara N, Gerber HP, et al. The hypoxic response of tumors is dependent on their microenvironment. Cancer Cell. 2003; 4:133–146. [PubMed: 12957288]

17. Carmeliet P, Dor Y, Herbert JM, Fukumura D, Brusselmans K, Dewerchin M, et al. Role of HIF-1alpha in hypoxia-mediated apoptosis, cell proliferation and tumour angiogenesis. Nature. 1998; 394:485–490. [PubMed: 9697772]

18. Rankin EB, Giaccia AJ. The role of hypoxia-inducible factors in tumorigenesis. Cell Death Differ. 2008; 15:678–685. [PubMed: 18259193]

19. Chu RL, Post DE, Khuri FR, Van Meir EG. Use of replicating oncolytic adenoviruses in combination therapy for cancer. Clin Cancer Res. 2004; 10:5299–5312. [PubMed: 15328165]

20. Jiang H, McCormick F, Lang FF, Gomez-Manzano C, Fueyo J. Oncolytic adenoviruses as antiglioma agents. Expert Rev Anticancer Ther. 2006; 6:697–708. [PubMed: 16759161]

21. Glasgow JN, Bauerschmitz GJ, Curiel DT, Hemminki A. Transductional and transcriptional targeting of adenovirus for clinical applications. Curr Gene Ther. 2004; 4:1–14. [PubMed: 15032610]

22. Alemany R. Cancer selective adenoviruses. Mol Aspects Med. 2007; 28:42–58. [PubMed: 17300834]

23. Post DE, Shim H, Toussaint-Smith E, Van Meir EG. Cancer scene investigation: how a cold virus became a tumor killer. Future Oncol. 2005; 1:247–258. [PubMed: 16555996]

24. Bischoff JR, Kirn DH, Williams A, Heise C, Horn S, Muna M, et al. An adenovirus mutant that replicates selectively in p53-deficient human tumor cells. Science. 1996; 274:373–376. [PubMed: 8832876]

25. Rothmann T, Hengstermann A, Whitaker NJ, Scheffner M, zur Hausen H. Replication of ONYX-015, a potential anticancer adenovirus, is independent of p53 status in tumor cells. J Virol. 1998; 72:9470–9478. [PubMed: 9811680]

26. Goodrum FD, Ornelles DA. p53 status does not determine outcome of E1B 55-kilodalton mutant adenovirus lytic infection. J Virol. 1998; 72:9479–9490. [PubMed: 9811681]

27. Post DE, Van Meir EG. Generation of bidirectional hypoxia/HIF-responsive expression vectors to target gene expression to hypoxic cells. Gene Ther. 2001; 8:1801–1807. [PubMed: 11803400]

28. Post DE, Van Meir EG. A novel hypoxia-inducible factor (HIF) activated oncolytic adenovirus for cancer therapy. Oncogene. 2003; 22:2065–2072. [PubMed: 12687009]

29. Post DE, Devi NS, Li Z, Brat DJ, Kaur B, Nicholson A, et al. Cancer therapy with a replicating oncolytic adenovirus targeting the hypoxic microenvironment of tumors. Clin Cancer Res. 2004; 10:8603–8612. [PubMed: 15623644]

30. Okada H, Kuwashima N. Gene therapy and biologic therapy with interleukin-4. Curr Gene Ther. 2002; 2:437–450. [PubMed: 12477255]

31. Post DE, Sandberg EM, Kyle MM, Devi NS, Brat DJ, Xu Z, et al. Targeted cancer gene therapy using a hypoxia inducible factor dependent oncolytic adenovirus armed with interleukin-4. Cancer Res. 2007; 67:6872–6881. [PubMed: 17638898]

32. Arany Z, Huang LE, Eckner R, Bhattacharya S, Jiang C, Goldberg MA, et al. An essential role for p300/CBP in the cellular response to hypoxia. Proc Natl Acad Sci U S A. 1996; 93:12969–12973. [PubMed: 8917528]

33. Saito Y, Sunamura M, Motoi F, Abe H, Egawa S, Duda DG, et al. Oncolytic replication-competent adenovirus suppresses tumor angiogenesis through preserved E1A region. Cancer Gene Ther. 2006; 13:242–252. [PubMed: 16179928]

34. Gallimore PH, Turnell AS. Adenovirus E1A: remodelling the host cell, a life or death experience. Oncogene. 2001; 20:7824–7835. [PubMed: 11753665]

35. Kramer PR, Stringer JR, Sinden RR. Stability of an inverted repeat in a human fibrosarcoma cell. Nucleic Acids Res. 1996; 24:4234–4241. [PubMed: 8932378]

36. Lobachev KS, Shor BM, Tran HT, Taylor W, Keen JD, Resnick MA, et al. Factors affecting inverted repeat stimulation of recombination and deletion in Saccharomyces cerevisiae. Genetics. 1998; 148:1507–1524. [PubMed: 9560370]

37. Bissler JJ. DNA inverted repeats and human disease. Front Biosci. 1998; 3:d408–d418. [PubMed: 9516381]

38. Lichtenstein DL, Toth K, Doronin K, Tollefson AE, Wold WS. Functions and mechanisms of action of the adenovirus E3 proteins. Int Rev Immunol. 2004; 23:75–111. [PubMed: 14690856]

39. Tollefson AE, Scaria A, Hermiston TW, Ryerse JS, Wold LJ, Wold WS. The adenovirus death protein (E3-11.6K) is required at very late stages of infection for efficient cell lysis and release of adenovirus from infected cells. J Virol. 1996; 70:2296–2306. [PubMed: 8642656]

40. Hawkins LK, Johnson L, Bauzon M, Nye JA, Castro D, Kitzes GA, et al. Gene delivery from the E3 region of replicating human adenovirus: evaluation of the 6.7 K/gp19 K region. Gene Ther. 2001; 8:1123–1131. [PubMed: 11509942]

41. Hawkins LK, Hermiston TW. Gene delivery from the E3 region of replicating human adenovirus: evaluation of the ADP region. Gene Ther. 2001; 8:1132–1141. [PubMed: 11509943]

42. Hawkins LK, Hermiston T. Gene delivery from the E3 region of replicating human adenovirus: evaluation of the E3B region. Gene Ther. 2001; 8:1142–1148. [PubMed: 11509944]

43. Bortolanza S, Bunuales M, Alzuguren P, Lamas O, Aldabe R, Prieto J, et al. Deletion of the E3-6.7K/gp19K region reduces the persistence of wild-type adenovirus in a permissive tumor model in Syrian hamsters. Cancer Gene Ther. 2009

44. Kasper LH, Boussouar F, Boyd K, Xu W, Biesen M, Rehg J, et al. Two transactivation mechanisms cooperate for the bulk of HIF-1-responsive gene expression. EMBO J. 2005; 24:3846–3858. [PubMed: 16237459]

45. Lisy K, Peet DJ. Turn me on: regulating HIF transcriptional activity. Cell Death Differ. 2008; 15:642–649. [PubMed: 18202699]

46. Cho WK, Seong YR, Lee YH, Kim MJ, Hwang KS, Yoo J, et al. Oncolytic effects of adenovirus mutant capable of replicating in hypoxic and normoxic regions of solid tumor. Mol Ther. 2004; 10:938–949. [PubMed: 15509511]

47. Shen BH, Hermiston TW. Effect of hypoxia on Ad5 infection, transgene expression and replication. Gene Ther. 2005; 12:902–910. [PubMed: 15690062]

48. Pipiya T, Sauthoff H, Huang YQ, Chang B, Cheng J, Heitner S, et al. Hypoxia reduces adenoviral replication in cancer cells by downregulation of viral protein expression. Gene Ther. 2005; 12:911–917. [PubMed: 15690061]

49. Toth K, Spencer JF, Tollefson AE, Kuppuswamy M, Doronin K, Lichtenstein DL, et al. Cotton rat tumor model for the evaluation of oncolytic adenoviruses. Hum Gene Ther. 2005; 16:139–146. [PubMed: 15703497]

50. Hallden G, Hill R, Wang Y, Anand A, Liu TC, Lemoine NR, et al. Novel immunocompetent murine tumor models for the assessment of replication-competent oncolytic adenovirus efficacy. Mol Ther. 2003; 8:412–424. [PubMed: 12946314]

51. Wang Y, Hallden G, Hill R, Anand A, Liu TC, Francis J, et al. E3 gene manipulations affect oncolytic adenovirus activity in immunocompetent tumor models. Nat Biotechnol. 2003; 21:1328–1335. [PubMed: 14555956]

52. Guo W, Zhu H, Zhang L, Davis J, Teraishi F, Roth JA, et al. Combination effect of oncolytic adenovirotherapy and TRAIL gene therapy in syngeneic murine breast cancer models. Cancer Gene Ther. 2006; 13:82–90. [PubMed: 16037823]

53. Stanford MM, McFadden G. The 'supervirus'? Lessons from IL-4-expressing poxviruses. Trends Immunol. 2005; 26:339–345. [PubMed: 15922951]

54. Fischer JE, Johnson JE, Kuli-Zade RK, Johnson TR, Aung S, Parker RA, et al. Overexpression of interleukin-4 delays virus clearance in mice infected with respiratory syncytial virus. J Virol. 1997; 71:8672–8677. [PubMed: 9343225]

55. Moran TM, Isobe H, Fernandez-Sesma A, Schulman JL. Interleukin-4 causes delayed virus clearance in influenza virus-infected mice. J Virol. 1996; 70:5230–5235. [PubMed: 8764032]

56. Benedetti S, Bruzzone MG, Pollo B, Dimeco F, Magrassi L, Pirola B, et al. Eradication of rat malignant gliomas by retroviral-mediated, in vivo delivery of the interleukin 4 gene. Cancer Res. 1999; 59:645–652. [PubMed: 9973213]

57. Saleh M, Wiegmans A, Malone Q, Stylli SS, Kaye AH. Effect of in situ retroviral interleukin-4 transfer on established intracranial tumors. J Natl Cancer Inst. 1999; 91:438–445. [PubMed: 10070943]

58. Bortolanza S, Bunuales M, Otano I, Gonzalez-Aseguinolaza G, Ortiz-de-Solorzano C, Perez D, et al. Treatment of pancreatic cancer with an oncolytic adenovirus expressing interleukin-12 in Syrian hamsters. Mol Ther. 2009; 17:614–622. [PubMed: 19223865]

59. Toth K, Spencer JF, Wold WS. Immunocompetent, semi-permissive cotton rat tumor model for the evaluation of oncolytic adenoviruses. Methods Mol Med. 2007; 130:157–168. [PubMed: 17401171]

60. Thomas MA, Spencer JF, Wold WS. Use of the Syrian hamster as an animal model for oncolytic adenovirus vectors. Methods Mol Med. 2007; 130:169–183. [PubMed: 17401172]

61. Ishii N, Maier D, Merlo A, Tada M, Sawamura Y, Diserens AC, et al. Frequent co-alterations of *TP53*, *p16/CDKN2A*, *p14*^{ARF}, *PTEN* tumor suppressor genes in human glioma cell lines. Brain Pathol. 1999; 9:469–479. [PubMed: 10416987]
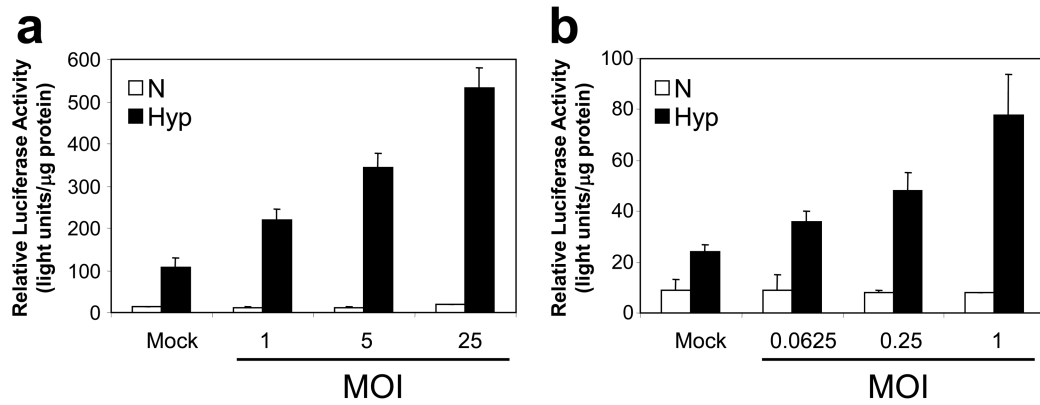
Figure 1. The Ad replication cycle further increases HIF transcriptional activity under hypoxia rather than inhibiting its activity

LN229 (**a**) and U251MG-T2 (**b**) cells were transfected with the pBIGL-V6R plasmid which contains a luciferase reporter gene under the regulation of a HIF-responsive promoter. Cells were then infected with a wild-type Ad (dl309-Ad) at the indicated multiplicity of infection (MOI) and incubated under normoxia versus hypoxia. The next day, luciferase activity was measured and normalized to total cellular protein levels (light units/µg protein). The data represent the mean ± SD.
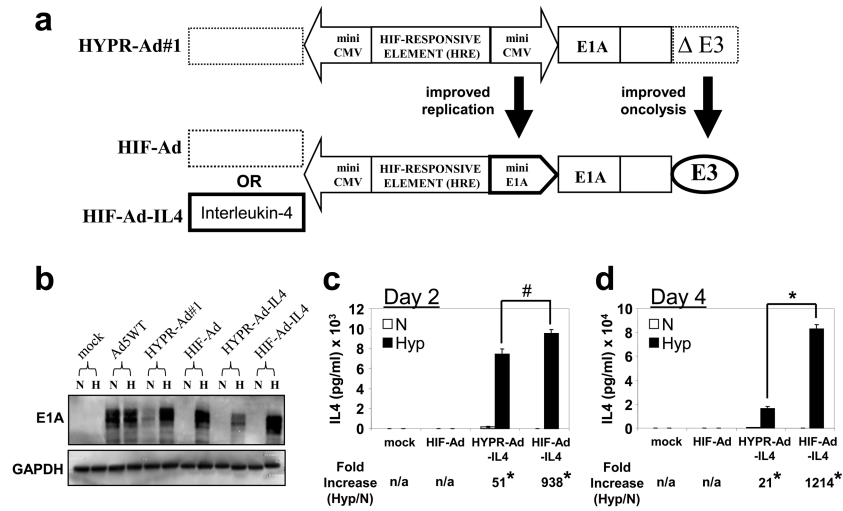
Figure 2. Hypoxia-dependent E1A and IL4 expression by HIF-Ad and HIF-Ad-IL4
(a) Schematic of HYPR-Ad and HIF-Ad. HYPR-Ad#1 contains a bi-directional HIF-responsive promoter composed of a HIF-responsive element (HRE) flanked by two opposing minimal CMV promoters [28]. In HIF-Ad, the HIF-responsive element is flanked by two genetically distinct minimal promoters; CMV and the endogenous E1A. In both viruses, the right arm of the promoter regulates the E1A replication gene. HYPR-Ad#1 contains a deletion of the E3 region (E3) whereas HIF-Ad contains an intact E3 region (E3). The dotted boxes in HYPR-Ad#1 and HIF-Ad represent a multiple cloning site for the incorporation of an adjuvant therapy gene in the left arm of the bi-directional HIF-promoter. In HIF-Ad-IL4, the interleukin-4 cDNA was inserted into the left arm of the HIF-promoter. **(b-c)** LN229 cells were mock or virus infected at MOI 1 and then grown under normoxia versus hypoxia. **(b)** Total cell lysates were examined by western blot analysis for Ad E1A and cellular GAPDH (loading control) at 3 days post infection (dpi). **(c,d)** IL4 in the conditioned media was measured by ELISA at 2 **(c)** and 4 **(d)** dpi. The data represent the mean ± SD. Asterisks indicate a significant increase in IL4 levels under hypoxia compared to normoxia ($p < 0.001$). The number sign (#) indicates no significant difference in IL4 levels under hypoxia ($p > 0.951$).
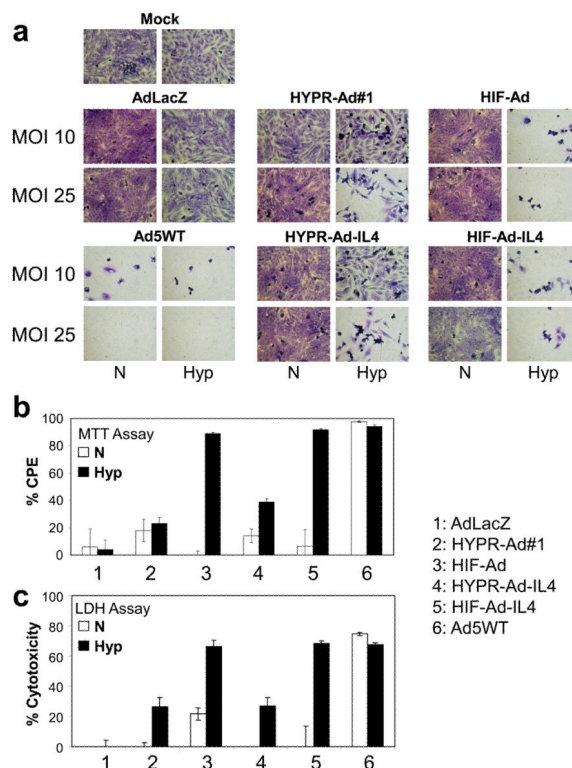
Figure 3. The HIF-Ads have dramatically improved hypoxia-dependent oncolytic activity compared to the HYPR-Ads

(a) <u>CPE Assay.</u> LN229 tumor cells were mock or virus infected at MOI 10 or 25 and then maintained under normoxia versus hypoxia. Cells were visually monitored for CPE (cytolysis/detachment). Shown are photographs (100X magnification) of crystal violet stained cells taken 6 dpi. **(b)** <u>MTT Assay.</u> LN229 cells were mock or virus infected at MOI 25 and then maintained under normoxia versus hypoxia. CPE was measured by an MTT assay at 8 dpi. The percent CPE obtained with each virus was normalized to mock infected cells. This data represents the mean ± SD of two independent experiments. **(c)** <u>LDH Assay.</u> LN229 cells were mock or virus infected at MOI 25 and then maintained under normoxia vs. hypoxia. Cytotoxicity was evaluated by an LDH assay at 3 dpi. The cytotoxicity observed with each virus was normalized to mock infected cells. The data represent the mean ± SD.
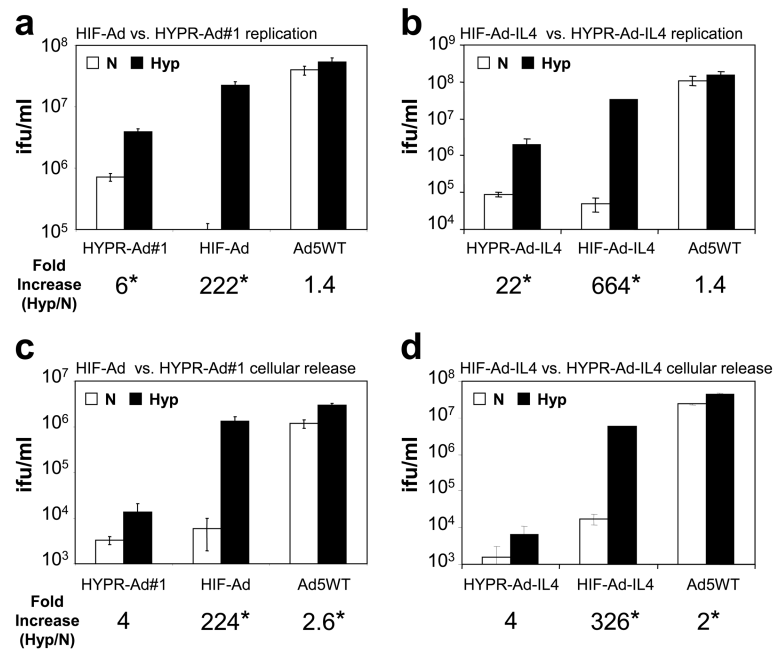
Figure 4. The HIF-Ads have significantly improved hypoxia-dependent replication and cellular release compared to the HYPR-Ads

LN229 cells were infected with the indicated virus at MOI 1 and then grown under normoxia vs. hypoxia. **(a, b)** Virus replication was examined at 2 dpi by titering the amount of virus in total cell lysates. The data represent the mean ± SD. Asterisks indicate a significant increase in virus replication under hypoxia compared to normoxia (Hyp/N, $p<0.05$). **(c, d)** Cellular release was examined at 2 dpi by titering the amount of virus in conditioned media. The data represent the mean ± SD. Asterisks indicate a significant increase in cellular release under hypoxia compared to normoxia (Hyp/N, $p<0.05$).
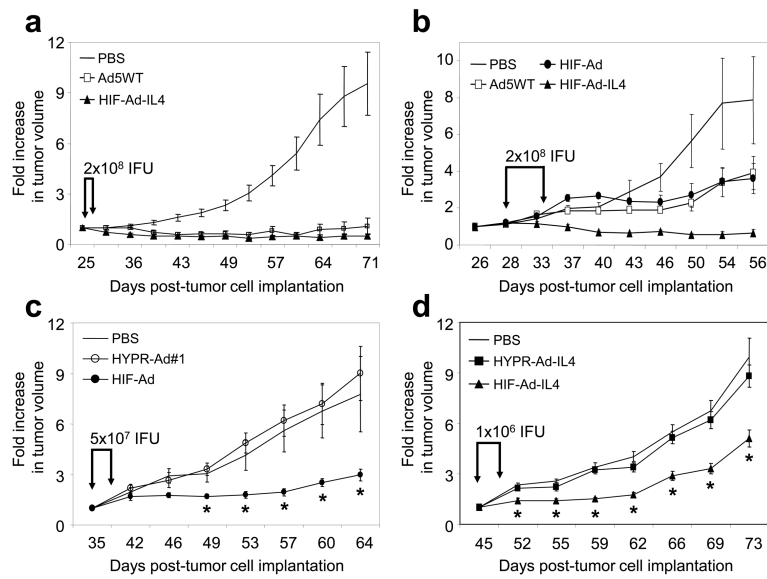
Figure 5. HIF-Ad and HIF-Ad-IL4 have anti-tumor activity <u>which is superior to the HYPR-Ads</u>
LN229 tumor xenografts were established subcutaneously in *nu/nu* mice (Day 1). **(a)**
Tumors (average size of 92 mm^3) were intratumorally injected with 2×10^8 IFU of HIF-Ad-
IL4, Ad5WT or PBS on Days 26 and 29. n=10 mice/group. **(b)** Tumors (average size of 235
mm^3) were intratumorally injected with 2×10^8 IFU of HIF-Ad, HIF-Ad-IL4, Ad5WT or
PBS on Days 28 and 34. n=4 mice/group. **(c)** Tumors (average size of 110 mm^3) were
intratumorally injected with 5×10^7 IFU of HIF-Ad (n=9), HYPR-Ad#1 (n=9), or PBS
(n=8) on Days 35 and 39. **(d)** Tumors (average size of 226 mm^3) were intratumorally
injected with 1×10^6 IFU of HIF-Ad-IL4 (n=8), HYPR-Ad-IL4 (n=9), or PBS (n=8) on Days
45 and 49. Tumor growth was monitored by caliper measurement. The data represent the
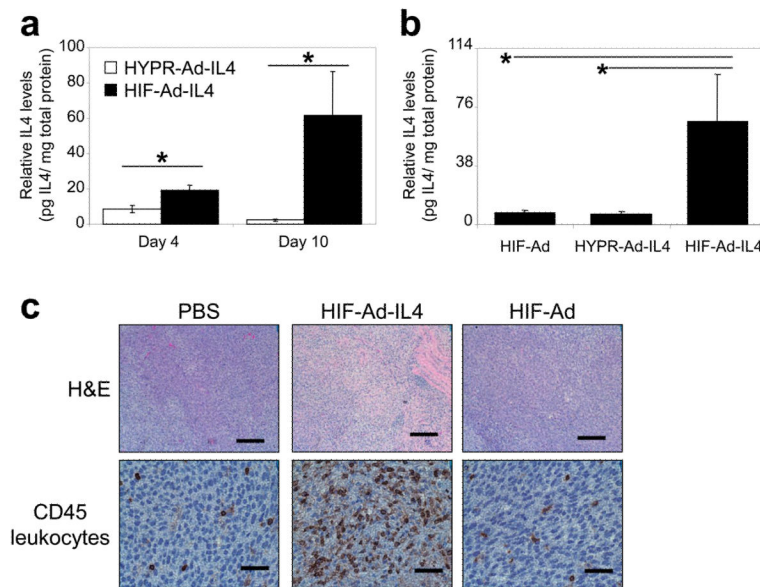mean ± SEM.

Figure 6. HIF-Ad-IL4 expresses high levels of IL4 intratumorally and induces tumor infiltration by CD45+ leukocytes

LN229 tumor xenografts were established subcutaneously in *nu/nu* mice. **(a)** Tumors (n=5/group) were established to an average size of 223 mm^3, intratumorally injected with 5×10^5 IFU of HYPR-Ad-IL4 or HIF-Ad-IL4, and then collected at Days 4 and 10 post-treatment. **(b)** Tumors (n=6/group) were established to an average size of 132 mm^3, intratumorally injected with 5×10^5 IFU of HIF-Ad, HYPR-Ad-IL4, or HIF-Ad-IL4, and then collected at Day 11 post-treatment. **(a, b)** Intratumoral IL4 protein levels were measured by ELISA and then normalized to total protein levels in cleared tumor homogenates. The data represent the mean ± SEM. Asterisks indicate a significant increase in intratumoral IL4 levels ($p < 0.033$). **(c)** Tumors were intratumorally injected with PBS or 1×10^7 IFU of HIF-Ad or HIF-Ad-IL4 at Days 35 and 39 post tumor cell implantation. Fourteen days from the start of virus treatment (Day 49), tumors were harvested and stained with H&E or immunostained for CD45 leukocyte common antigen, a pan-leukocyte marker. Magnifications are 100x for H&E and 400X for CD45. The black scale bar is 200 microns for H&E and 50 microns for CD45.